International Communications in Heat and Mass Transfer 39 (2012) 282–290

Contents lists available at SciVerse ScienceDirect

International Communications in Heat and Mass Transfer

journal homepage: www.elsevier.com/locate/ichmt

Natural convection for hot materials confined within two entrapped porous trapezoidal cavities ☆

Yasin Varol *

Department of Automotive Engineering, Technology Faculty, Firat University, 23119 Elazig, Turkey

ARTICLE INFO

Available online 18 November 2011

Keywords:
Entrapped trapezoidal cavity
Natural convection
Heat recovery

ABSTRACT

This paper analyzes the detailed heat transfer and fluid flow within two entrapped porous trapezoidal cavities involving cold inclined walls and hot horizontal walls. Flow patterns and temperature distribution were obtained by solving numerically the governing equations, using Darcy's law. Results are presented for different values of the governing parameters, such as Darcy-modified Rayleigh number, aspect ratio of two entrapped trapezoidal cavities and thermal conductivity ratio between the middle horizontal wall and fluid medium. Heat transfer rates are estimated in terms of local and mean Nusselt numbers. Local Nusselt numbers with spatial distribution exhibit monotonic trend irrespective of all Rayleigh numbers for the upper trapezoidal whereas wavy distribution of local Nusselt number occur for the lower trapezoidal.

1. Introduction

Indirect heat transfer of fluids plays an important role in people's lives [1–5]. It also has various applications in, for instance, material industries, geophysical processes, pollution control, food processing, etc. [6–9]. Heat exchangers have also been benefited in various environmental applications such as thermal pollution, air pollution, and water pollution. They are also very critical for energy conservation, conversion, recovery and successful implementation of new energy sources, and wide usage of it involves food processing, power transportation, air-conditioning and refrigeration, heat recovery, alternate fuels, etc. [10–16]. There exist two ways to analyze these applications: experimental and numerical methods. The latter is the most preferred way due to the high cost involved in experiments.

The present study analyzes the heat recovery of entrapped fluid between a stack of tubes, shown in Fig. 1a. The cold fluid passing through the stack of tubes may recover excessive heat associated with the hot fluid during the material processing. The application of the current study is given as follows: consider an assembly of diamond shaped tubes adjacent to each other and the space between two adjacent tubes is two porous trapezoidal cavities with entrapped fluid. Cold fluid may be pumped through the tubes to recover heat from hot entrapped fluid. This study examines the complete heat transfer in entrapped porous trapezoidal cavities in detail. Fig. 1b shows the computational domain with associated boundary conditions. The length of the bottom wall was L and height of the cavity was $H = L/2$.

Natural convection is important for thermal processing based on various applications [17]. In the literature, there are several studies on natural convection flows in porous trapezoidal cavities. The study for inclined trapezoidal enclosure at different inclination angles filled with a viscous fluid has been analyzed by Lee [18]. He made a numerical study to analyze the natural convection heat transfer in an inclined trapezoidal enclosure filled with a viscous fluid for different Prandtl numbers using body-fitted coordinate systems. It was shown that the heat transfer in a trapezoidal enclosure with two symmetrical, inclined sidewalls of moderate aspect ratio was a strong function of the orientation angle of the cavity.

Kumar and Kumar [19] used parallel computation technique to analyze the natural convection heat transfer in a trapezoidal enclosure filled with a porous medium. The short bottom and the long top walls are taken adiabatic, while the sloping walls are differentially heated. They showed that the inclination of the side wall significantly affects the flow and temperature distribution. Baytas and Pop [20] solved to Darcy and energy equation in cylindrical coordinates using ADI method to analyze natural convection in a trapezoidal enclosure filled with a porous medium. It has been observed that up to Rayleigh number, $Ra = 100$, a conduction-dominated regime prevails, and afterwards a two-cellular convective flow regime takes place at the tilt angle 165°. Moukalled and Acharya [21] studied the conjugate natural convection in a trapezoidal enclosure with a divider attached inclined wall and filled with a viscous fluid. Moukalled and Darwish [22] made a numerical work on natural convection in a partitioned trapezoidal cavity using the special momentum-weighted interpolation method. They used conductive partition and showed that the presence of baffles decrease heat transfer as high as 70%. Other similar studies on natural convection in trapezoidal enclosures can be found in Peric [23], Van Der Eyden et al. [24], Boussaid et al. [25], Kumar [26], Papanicolaou and Belessiotis [27], Hammami et al. [28], Varol et al. [29–32], Natarajan et al. [33] and Basak et al. [34].

☆ Communicated by W.J. Minkowycz.

* Visiting professor, Tennessee State University, Department of Computer Science, Nashville, TN 37209, USA.
E-mail address: ysnvarol@gmail.com.

0735-1933/$ – see front matter © 2011 Elsevier Ltd. All rights reserved.
doi:10.1016/j.icheatmasstransfer.2011.11.005

Nomenclature

AR	aspect ratio of two entrapped trapezoidal cavities, $\ell x/L$
g	gravitational acceleration
H	height of the cavity, $H=L/2$
k_f	thermal conductivity of the fluid
k_s	thermal conductivity of the middle horizontal wall
k	thermal conductivity ratio, (k_s/k_f)
K	permeability of the porous medium
L	dimensionless length of bottom or top horizontal walls
ℓx	dimensionless length of middle horizontal wall
Nu_x	local Nusselt number
Nu	mean Nusselt number
Pr	Prandtl number
Ra	Darcy-modified Rayleigh number
T	temperature
u, *v*	dimensional axial and radial velocities
X, *Y*	non-dimensional coordinates

Greek letters

α_m	effective thermal diffusivity of the porous medium
β	thermal expansion coefficient
θ	non-dimensional temperature
υ	kinematic viscosity
Ψ	non-dimensional stream function

Subscript

c	cold
f	fluid
h	hot
s	solid

Basak et al. [35] recently made a numerical study solving the momentum and energy equations within two entrapped porous triangular cavities involving cold inclined walls and hot horizontal walls using a penalty finite element analysis with bi-quadratic elements. The authors also conducted other studies with two entrapped non-porous triangular cavities for different boundary conditions [36,37].

As seen above, there has been a considerable amount of work on heat transfer within trapezoidal and two entrapped triangular cavities reported in the literature. This study differs from the other studies because it incorporates two entrapped trapezoidal cavities. The objective of the present investigation is to analyze the heat recovery from hot fluids passing parallel to the hot plates and heat may be transported to the entrapped fluid between a stack of tubes. Cold fluid may be pumped through the tubes to recover heat from hot entrapped fluid. The present investigation aims to study the complete heat transfer details in two entrapped porous trapezoidal cavities (Fig. 1a). The computational domain with associated boundary conditions is shown in Fig. 1(a) and (b). Streamlines, isotherms, and local and mean Nusselt numbers is presented in the following sections of the paper for Darcy-modified Rayleigh number, aspect ratio of two entrapped trapezoidal cavities and thermal conductivity ratio between the middle horizontal wall and fluid medium.

2. Physical model and governing equations

A schematic of the in two entrapped porous trapezoidal cavities and grid arrangement is shown in Fig. 1(a) and (b), respectively. The cold fluid is pumped through the hexagonal tubes. The flow rate may be sufficiently high such that cold fluid may act as a sink and the inclined wall is maintained at a constant cold temperature. The horizontal top and bottom walls are maintained hot. The constant temperature at the hot wall is due to the flow of hot gases over the top wall and below the bottom wall.

Governing equations are written as follows:

$$\frac{\partial u}{\partial x}+\frac{\partial v}{\partial y}=0 \tag{1}$$

$$\frac{\partial u}{\partial y}-\frac{\partial v}{\partial x}=-\frac{g\beta K}{\upsilon}\frac{\partial T_f}{\partial x} \tag{2}$$

$$u\frac{\partial T_f}{\partial x}+v\frac{\partial T_f}{\partial y}=\alpha_m\left(\frac{\partial^2 T_f}{\partial x^2}+\frac{\partial^2 T_f}{\partial y^2}\right) \tag{3}$$

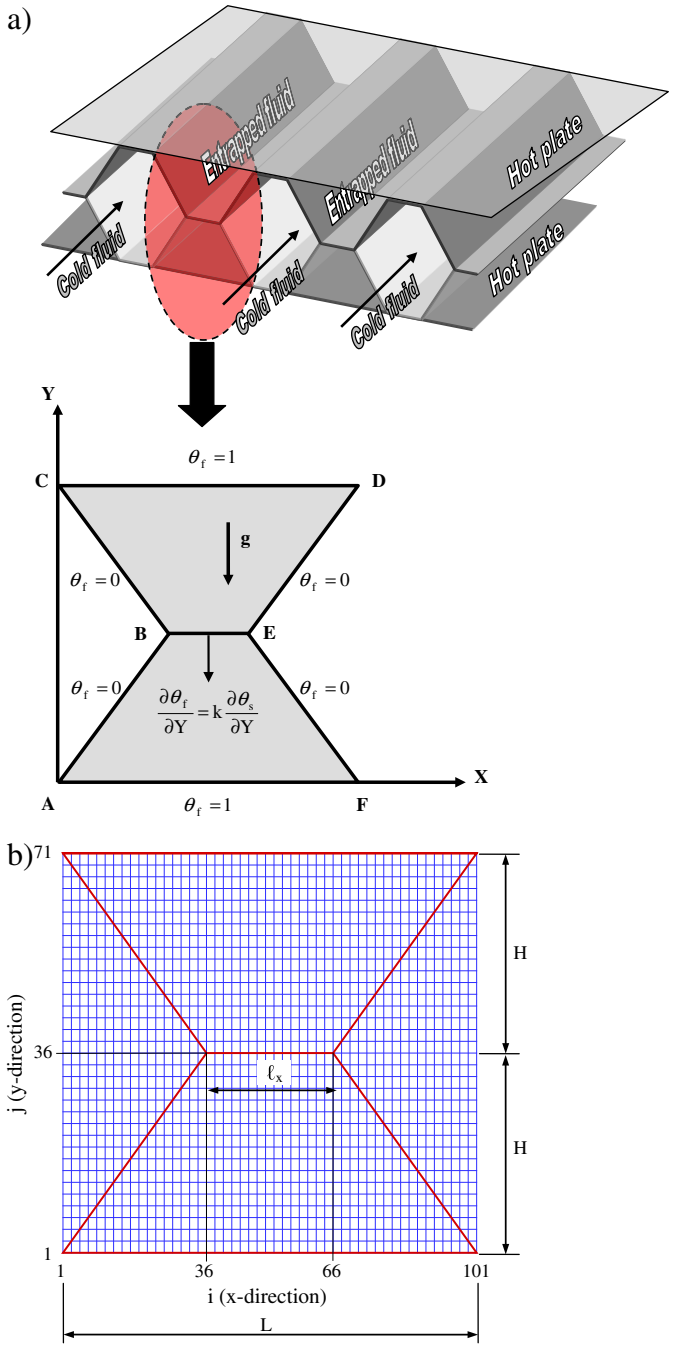

Fig. 1. a) Schematic diagram of the physical system and computational domain with the boundary conditions, and b) finite-difference grid for the computational domain.

and the energy equation for the middle horizontal wall are:

$$\frac{\partial^2 T_s}{\partial x^2}+\frac{\partial^2 T_s}{\partial y^2}=0. \tag{4}$$

To write the above equations the assumptions are listed as follows:

- the properties of the fluid and the porous medium are constant,
- the cavity walls are impermeable,
- the Boussinesq approximation and the Darcy law model are valid,
- the viscous drag and inertia terms in the Darcy and Energy equations are negligible.

In equations, u and v are the velocity components along x and y axes, T_f is the fluid temperature, g is the acceleration due to gravity, T_s is the temperature of the solid partition wall, K is the permeability of the porous medium, α_m is the effective thermal diffusivity of the porous medium, β is the thermal expansion coefficient and υ is the kinematic viscosity. Introducing the stream function ψ defined as

$$u=\frac{\partial \psi}{\partial y}, v=-\frac{\partial \psi}{\partial x}. \tag{5}$$

Eqs. (1)–(4) can be written in non-dimensional form as

$$\frac{\partial^2 \Psi}{\partial X^2}+\frac{\partial^2 \Psi}{\partial Y^2}=-Ra\frac{\partial \theta_f}{\partial X} \tag{6}$$

$$\frac{\partial \Psi}{\partial Y}\frac{\partial \theta_f}{\partial X}-\frac{\partial \Psi}{\partial X}\frac{\partial \theta_f}{\partial Y}=\frac{\partial^2 \theta_f}{\partial X^2}+\frac{\partial^2 \theta_f}{\partial Y^2} \tag{7}$$

for the interface between lower and upper trapezoidal cavity

$$\frac{\partial^2 \theta_s}{\partial X^2}+\frac{\partial^2 \theta_s}{\partial Y^2}=0 \tag{8}$$

for the middle horizontal wall, respectively. Here $Ra=g\beta K(T_h-T_c)L/\alpha_m\upsilon$ is the Darcy-modified Rayleigh number for the porous medium and the non-dimensional quantities are defined as

$$X=\frac{x}{L}, Y=\frac{y}{L}, \psi=\frac{\psi}{\alpha_m}, \theta_f=\frac{T_f-T_c}{T_h-T_c}, \theta_s=\frac{T_s-T_c}{T_h-T_c} \tag{9}$$

The boundary conditions for streamline and temperature for the entrapped lower trapezoidal cavity are as follows (Fig. 1a),

$$\Psi=0;\theta_f=0 \text{ on AB;} \tag{10a}$$

$$\Psi=0;\theta_f=0 \text{ on EF}$$

$$\Psi=0;\theta_f=1 \text{ on AF.}$$

The boundary conditions for streamline and temperature for the entrapped upper trapezoidal cavity are as follows (Fig. 1a),

$$\Psi=0;\theta_f=0 \text{ on BC;} \tag{10b}$$

$$\Psi=0;\theta_f=0 \text{ on ED;}$$

$$\Psi=0;\theta_f=1 \text{ on CD;}$$

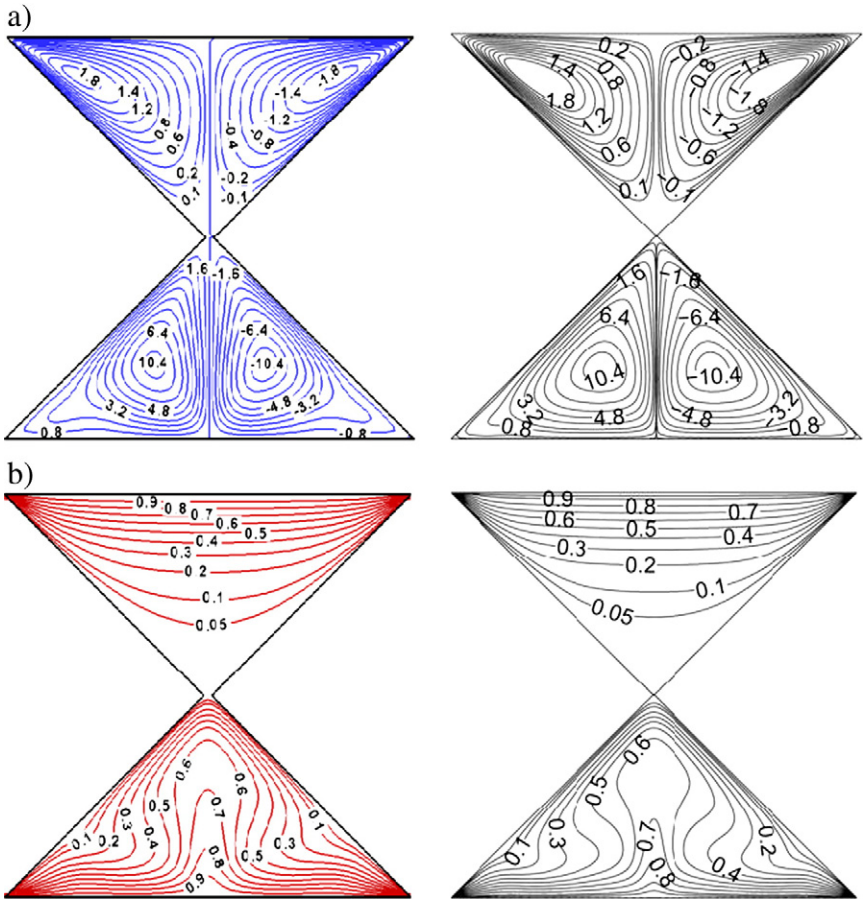

Fig. 2. Comparison of streamlines and isotherms with literature: a) streamlines for present (left) and Basak et al. [35] (right), b) isotherms for present (left) and Basak et al. [35] (right).

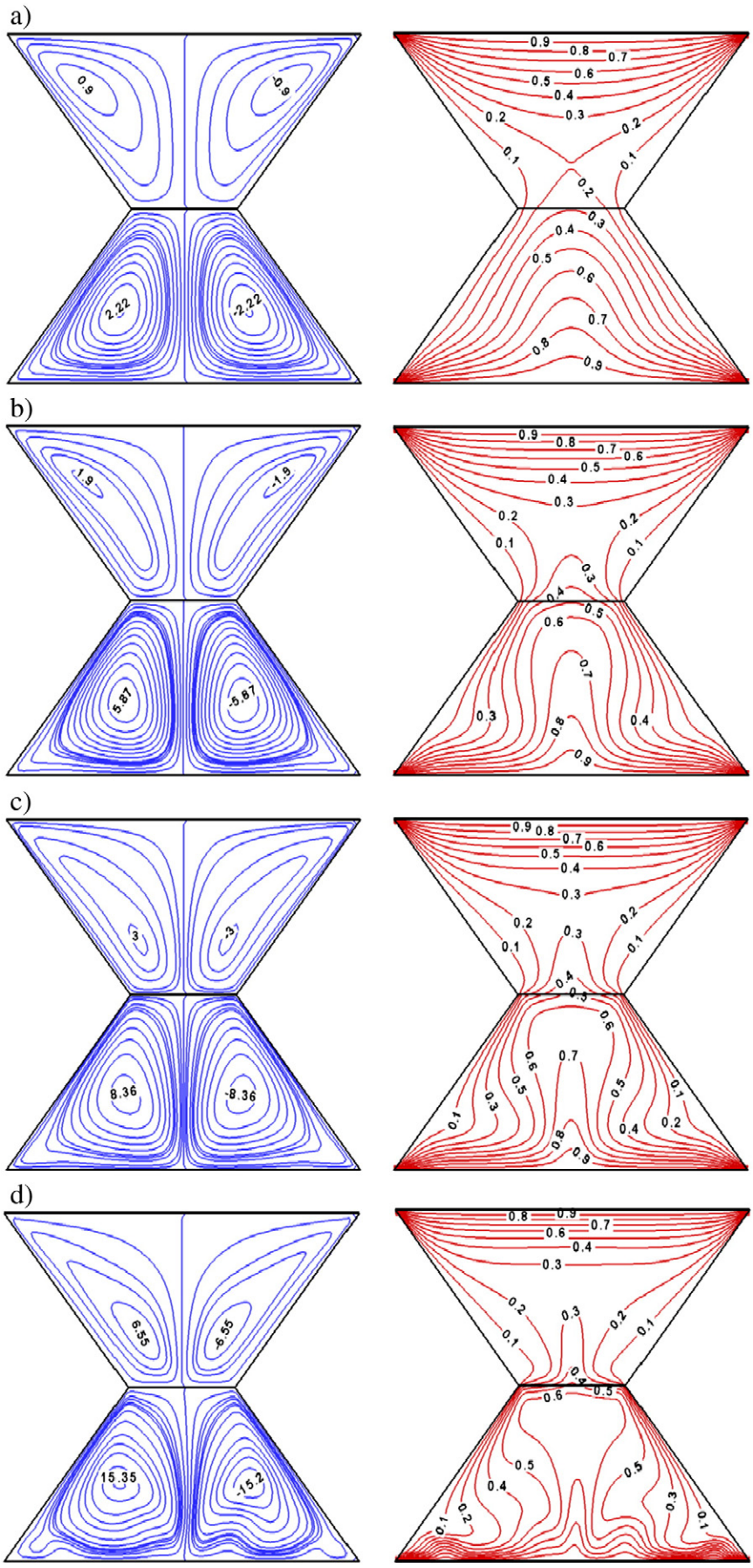

Fig. 3. Streamlines (left) and isotherms (right) for different Darcy-modified Rayleigh numbers at $AR = 0.3$ and $k = 1$, a) $Ra = 100$, b) $Ra = 250$, c) $Ra = 500$, and d) $Ra = 1000$.

for the interface between lower and upper trapezoidal cavity (Fig. 1a),

$$\Psi = 0; k_f \frac{\partial \theta_f}{\partial Y} = k_s \frac{\partial \theta_s}{\partial Y} \text{ on BE;} \tag{10c}$$

where k_f and k_s are the thermal conductivities of the fluid and middle horizontal wall, respectively. Physical quantities of interest in this problem are the local Nusselt number Nu_x and the mean Nusselt numberNu, which can be expressed as at the top horizontal wall:

$$Nu_x = \left(-\frac{\partial \theta_f}{\partial Y} \right)_{Y=1} \tag{11}$$

in the middle horizontal wall:

$$Nu_x = \left(-\frac{\partial \theta_f}{\partial Y} \right)_{Y=H} \tag{12}$$

at the bottom horizontal wall:

$$Nu_x = \left(-\frac{\partial \theta_f}{\partial Y} \right)_{Y=0} \quad , \quad Nu = \int_0^1 Nu \, dX \tag{13a, b}$$

Eqs. (6)–(8) were solved numerically with finite-difference method. Numerical simulations were carried out systematically in order to determine the effects of effective parameters of the problem as Darcy-modified Rayleigh Number Ra, thermal conductivity ratio between the middle horizontal wall and fluid medium $k(=k_s/k_f)$ and aspect ratio of two entrapped trapezoidal cavities, $AR = \ell x/L$ on the flow and heat transfer characteristics. To solve the equations on inclined boundaries, the techniques of Asan and Namli [38] and Haese and Teubner [39] were followed. The used mesh treatment was depicted in Fig. 1(b). The inclined wall was approximated with staircase-like zigzag lines.

The solution domain consists of grid points at which equations are applied. To obtain grid free solution, different grid dimensions were obtained for each AR and the following grid dimensions were chosen: 101x91 for $AR=0.1$, 101x81 for $AR=0.2$ and 101x71 for $AR=0.3$. More detailed information can be found in earlier studies [31].

The iteration process was terminated when the following condition is satisfied

$$\sum_{i,j} \left| \frac{\Phi_{i,j}^m - \Phi_{i,j}^{m-1}}{\Phi_{i,j}^m} \right| \leq 10^{-5} \tag{14}$$

where m denoted the iteration step and Φ stood for either θ_f, θ_s or Ψ.

2.1. Validation of the code

For validation of the code, a study conducted by Basak et al. [35] was used. For the present study, for when AR gets closer to zero ($AR \rightarrow 0 (\ell x \rightarrow 0)$), it turns out to be two entrapped triangular cavity, which allowed the researcher to compare the results with the ones in Basak et al. [35]. Results are shown by streamlines and isotherms contour plots in Fig. 2. The test shows that the results obtained using the present code give good agreement with those from the literature and it can be used with great confidence for further calculations.

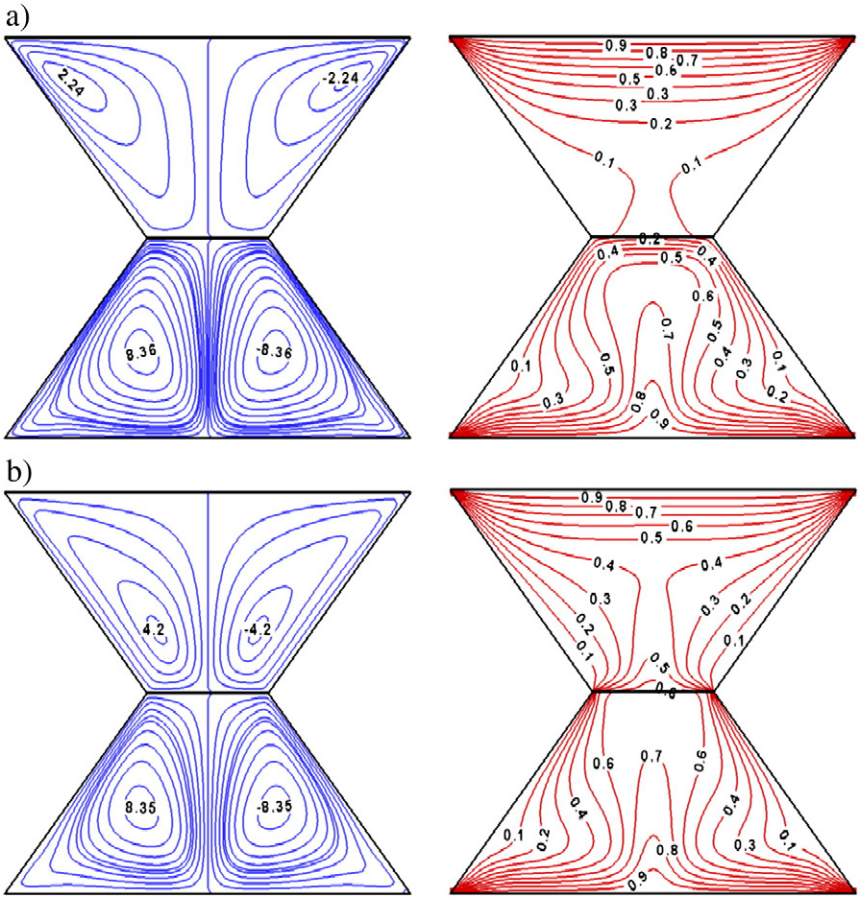

Fig. 4. Streamlines (left) and isotherms (right) for different thermal conductivity ratios at $AR=0.3$ and $Ra=500$, a) $k=0.1$ and b) $k=10$.

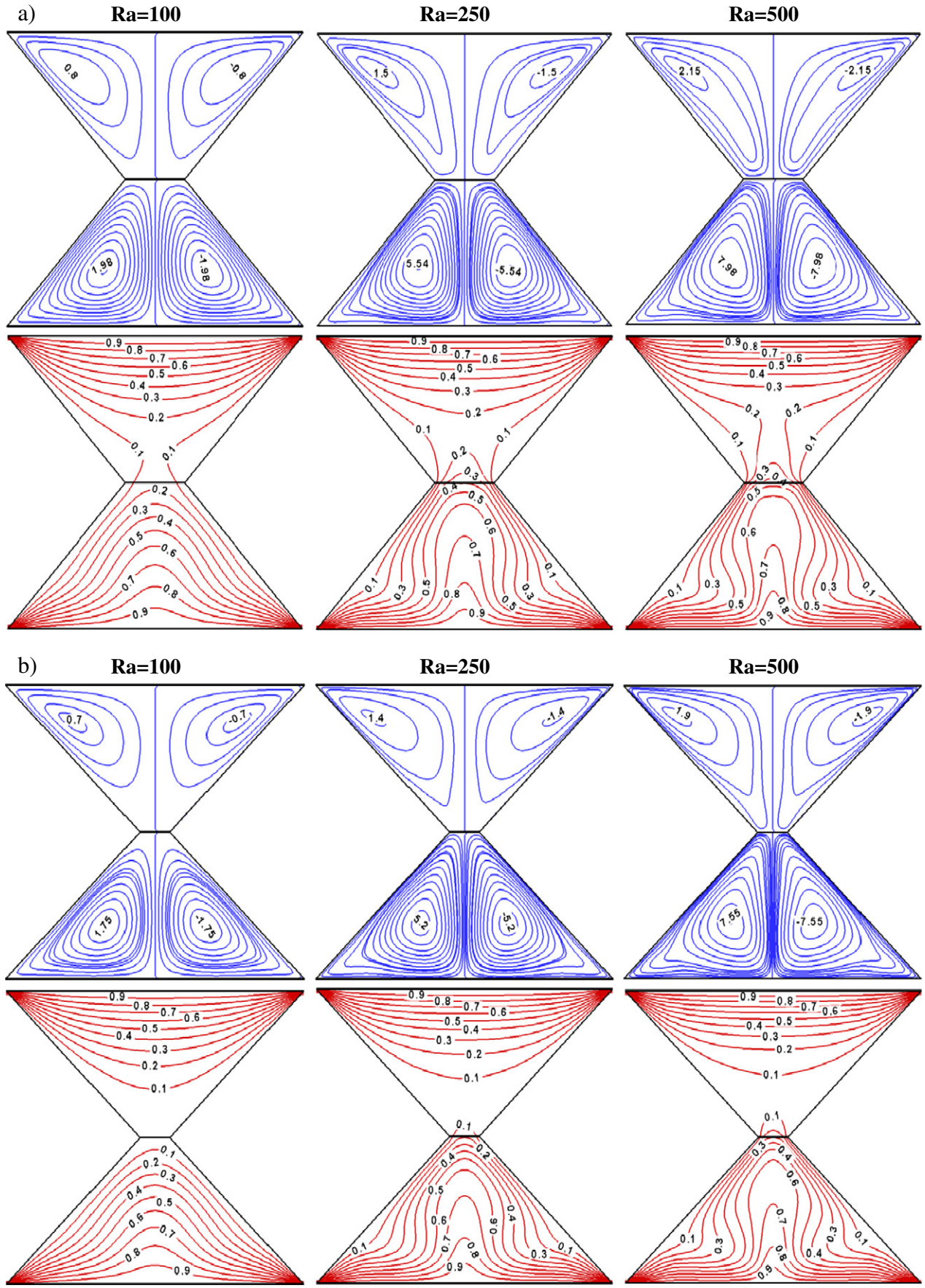

Fig. 5. Streamlines (top) and isotherms (bottom) for different aspect ratios at $k=1$, a) $AR=0.2$ and b) $AR=0.1$.

3. Results and discussion

In this study, numerical results for streamlines, isotherms, local and mean Nusselt numbers for natural convection in two entrapped porous trapezoidal cavity were obtained for Darcy-modified Rayleigh number, aspect ratio of two entrapped trapezoidal cavities and thermal conductivity ratio between the middle horizontal wall and fluid medium.

Fig. 3(a) to (d) shows the streamlines (on the left) and isotherms (on the right) for different Darcy-modified Rayleigh number at $AR=0.3$ and $k=1$. In these figures, four eddies were formed from $Ra=100$ to 1000. Fluid near the center of the horizontal bottom wall moves towards the top of the lower trapezoidal whereas fluid near the inclined wall tends to go down for the upper trapezoidal, forming a pair of symmetric circulations in different directions for both the cavities. The fluid circulations follow clockwise direction in the right half of the axis of symmetry and counterclockwise direction in the left half of the axis of symmetry. As expected, values of stream function was higher for below eddies than that of above eddies for all Darcy-modified Rayleigh numbers. At low values of the Darcy-modified Rayleigh number, Fig. 3(a), the isotherms for the upper trapezoidal are found to be smooth, monotonic whereas for the lower trapezoidal, the isotherms are distorted near the cold walls and at the central regime. It may be noted that the maximum value of the stream function is 0.9 for the upper trapezoidal whereas that was 2.22 for the lower trapezoidal. This illustrates that the heat transfer is primarily due to conduction. Flow strength increases with increasing of the Darcy-modified Rayleigh number due to increasing of heat transfer from hot wall to cold wall. The maximum values of stream function for upper trapezoidal are changed as 1.9, 3.0 and 6.55 for $Ra=250$, 500 and 1000, respectively whereas for the lower trapezoidal, the maximum values of stream function are change as 5.87, 8.36 and 15.35 (Fig. 3b–d). In this figure, the right column shows the temperature distribution. With increasing of the Darcy-modified Rayleigh number, the isotherms are largely deformed for the lower trapezoidal. The isotherms exhibit oscillatory pattern within the lower trapezoidal. For the highest Darcy-modified Rayleigh number, the plumelike flow was formed from bottom to top. On the other hand, for the upper trapezoidal, isotherms are highly compressed near the top wall. The stratification in isotherms has been observed in the upper trapezoidal. Thus, the influence of the Darcy-modified Rayleigh number for the fluid circulation within the upper trapezoidal is not significant.

Fig. 4(a) and (b) illustrates the effects of thermal conductivity for $AR=0.3$ and $Ra=500$ on flow fields and temperature distribution by plotting streamlines and isotherms, respectively. The results were given for the values of thermal conductivity for $k=0.1$ and 10. In the case, the flow strength increased with increasing of thermal conductivity values within the upper trapezoidal. The isotherms are compressed more at the middle horizontal wall for the lower trapezoidal. When k is equal to 0.1 the temperature at the core varies within 0.2–0.6. On the other hand, θ is found as 0.6–0.7 when k is 10. For the upper trapezoidal, the eye of vortices is moved towards at the middle horizontal wall. It is noted that, $\Psi_{max}=2.24$ for $k=0.1$ whereas $\Psi_{max}=4.2$ for $k=10$.

Fig. 5(a) and (b) illustrates the effects of the aspect ratio for $k=1$, $Ra=100$, 250 and 500 on flow fields and temperature distribution by plotting streamlines (on the top) and isotherms (on the bottom), respectively. Similar behavior of the flow and temperature field as in Fig. 3 is observed in these figures. However, the figure shows that the maximum values of the stream function decrease as the value of AR decreases. For $AR=0.2$ the maximum values of stream function for upper trapezoidal are changed as 0.8, 1.5 and 2.15 for $Ra=100$, 250 and 500, respectively whereas for the lower trapezoidal, the maximum values of stream function are changed to 1.98, 5.54 and 7.98. For $AR=0.1$ the maximum values of stream function for upper trapezoidal are changed as 0.7, 1.4 and 1.9 for $Ra=100$, 250 and 500, respectively whereas for the lower trapezoidal, the maximum values of stream function are change as 1.75, 5.2 and 7.55. The stratification in isotherms has been observed in the upper trapezoidal for all the Ra and AR. Thus, the influence of the Ra and AR for the fluid circulation within the upper trapezoidal is not significant. However, for $Ra=500$, the isotherms are compressed more at the middle horizontal wall for the lower trapezoidal and the temperature at the core varies within 0.5–0.6 for $AR=0.2$ whereas θ is found as 0.3–0.6 for $AR=0.1$.

Fig. 6(a) to (c) shows the variation of Nusselt number with the distance along the horizontal walls of the two entrapped trapezoidal cavities for different Darcy-modified Rayleigh numbers. As can be seen from the figures, distribution of local Nusselt number was completely symmetric according to middle axis of the all horizontal walls. In this context, Fig. 6(a) shows, due to high temperature gradients, the value of local Nusselt number is very high at the edges of the

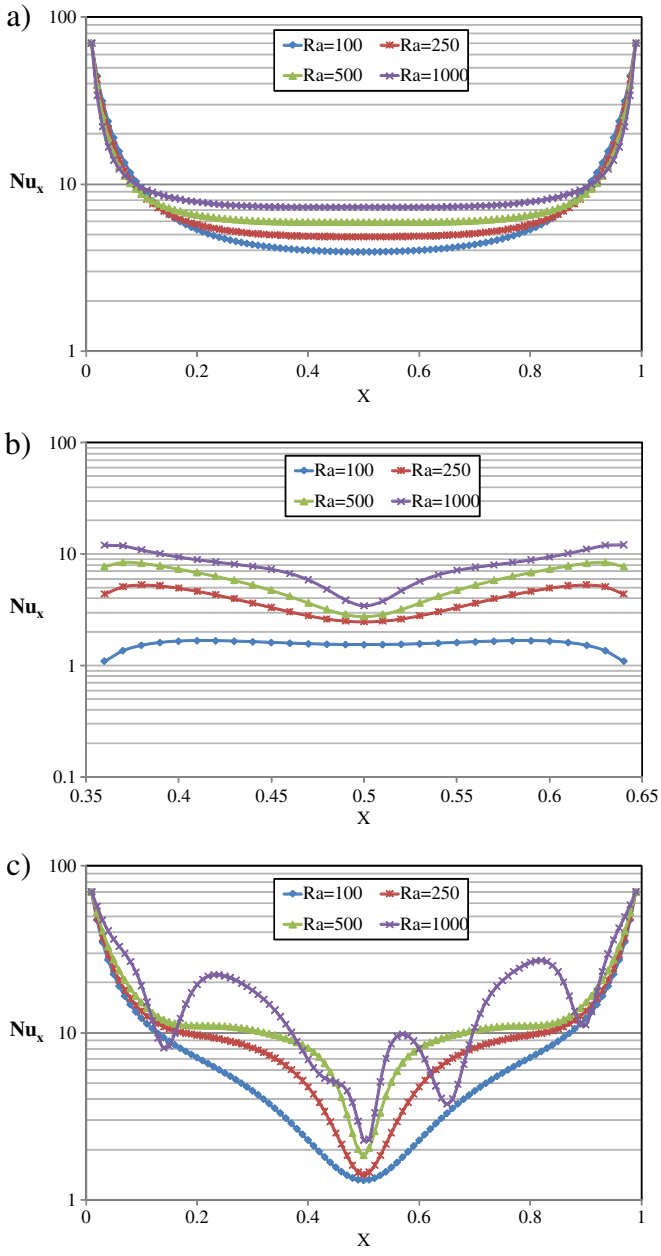

Fig. 6. The variation of local Nusselt number along the horizontal walls for different Darcy-modified Rayleigh numbers at $AR=0.3$ and $k=1$, a) along the top wall, b) along the middle wall, and c) along the bottom wall.

wall whilst the heat transfer rate reduces toward the center with nearly uniform values at the central region. The values of local Nusselt number increase monotonically with increasing of Darcy-modified Rayleigh number. The values of local Nusselt number are almost equal to each other for all Rayleigh numbers at $X=0.1$ and $X=0.9$. Fig. 6(b) shows the variation of Nusselt number with the distance along the middle horizontal wall. Values of local Nusselt number increase with increasing of Darcy-modified Rayleigh number and these values become constant along the middle horizontal wall. Fig. 6(c) shows the variation of Nusselt number with the distance along the bottom horizontal wall. It is observed that Nusselt number of the lower trapezoidal for $Ra=100$, 250 and 500 parabolic variations. Wavy variation of local Nusselt number is obtained for $Ra=1000$ due to increasing of convection heat transfer.

The overall heat transfer is presented via variation of mean Nusselt number and Darcy-modified Rayleigh number in Fig. 7 for different aspect ratios. As indicated in the figure, the mean Nusselt number is increased linearly with the increasing of the Darcy-modified Rayleigh number, which is an expected result. The value of mean Nusselt number becomes smaller with the increasing of aspect ratio because, in the case of higher aspect ratio, the length of the middle horizontal wall of the two entrapped trapezoidal cavity is increased. The highest mean Nusselt number value is obtained at the highest Darcy-modified Rayleigh number and the lowest value of aspect ratio.

4. Conclusions

Present study analyzes the details of natural convection heat transfer within two entrapped porous trapezoidal cavities which are enclosed between a pair of adjacent hexagonal tubes normally seen in heat recovery systems. The aim of this study is to analyze the efficient heat transfer details to the entrapped fluid in the system commonly used for practical applications in heat recovery during hot material processing. Equations of mass, momentum and energy have been written using Darcy law along with the Boussinesq approximation. Finite difference method was used to solve governing equations. The governing parameters were Darcy-modified Rayleigh number, aspect ratio of two entrapped trapezoidal cavities and thermal conductivity ratio between the middle horizontal wall and fluid medium. The conclusions derived from the present study may be listed as follows:

- Heat transfer increases with increasing of Darcy-modified Rayleigh number for all governing parameters.
- It is an interesting results that streamlines and isotherms contours become two entrapped porous trapezoidal cavities.

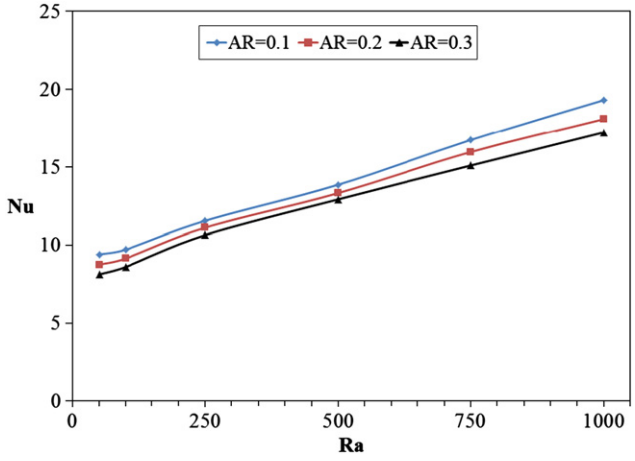

Fig. 7. Variation of mean Nusselt number with Darcy-modified Rayleigh number for different aspect ratios at $k=1$.

- The isotherms exhibit oscillatory pattern within the lower trapezoidal.
- The stratification in isotherms has been observed in the upper trapezoidal for all Darcy-modified Rayleigh numbers. Thus, the influence of the Darcy-modified Rayleigh number for the fluid circulation within the upper trapezoidal is not significant.
- The maximum mean Nusselt number is obtained for the highest Darcy-modified Rayleigh number and the lowest aspect ratio.

References

[1] R.K. Shah, D.P. Sekulic, Fundamentals of Heat Exchanger Design, John Wiley & Sons, 2007.
[2] D.B. Ingham, A. Bejan, E. Mamut, I. Pop, Emerging Technologies and Techniques in Porous Media, Kluwer, Dordrecht, 2004.
[3] Lei, J.C. Patterson, A direct three-dimensional simulation of radiation-induced natural convection in a shallow edge, International Journal Heat Mass Transfer 46 (2003) 1183–1197.
[4] K.A. Joudi, I.A. Hussein, A.A. Farhan, Computational model for a prism shaped storage solar collector with a right triangular cross section, Energy Conversion and Management 45 (2004) 391–409.
[5] A. Omri, J. Orfi, S. Ben Nasrallah, Natural convection effects in solar stills, Desalination 183 (2005) 173–178.
[6] J. Uhlir, Chemistry and technology of molten salts reactors-history and perspectives, Journal Nuclear Materials 360 (2007) 6–11.
[7] S.U. Rahman, Natural convection along vertical wavy surfaces: an experimental study, Chemical Engineering Journal 84 (2001) 587–591.
[8] R.A. Kuyper, T.H. Vandermeer, C.J. Hoogendoorn, Turbulent natural-convection flow due to combined buoyancy forces during underground gasification of thin coal layers, Chemical Engineering Science 49 (1994) 851–861.
[9] P.W. Cox, P.J. Fryer, Heat transfer to foods: modelling and validation, Journal Thermal Science 11 (2002) 320–330.
[10] L. Magistri, A. Traverso, A.F. Massardo, Heat exchangers for fuel cell and hybrid system applications, Journal Fuel cell Science Technology 3 (2006) 111–118.
[11] T.J. Sheer, G.B. De Klerk, H.H. Jawurek, M. Lander, A versatile computer simulation model for rotary regenerative heat exchangers, Heat Transfer Engineering 27 (2006) 68–79.
[12] J. Kragh, J. Rose, T.R. Nielsen, S. Svendsen, New counter flow heat exchanger designed for ventilation systems in cold climates, Energy and Buildings 39 (2007) 1151–1158.
[13] M. Nasif, R. Al-Waked, G. Morrison, M. Behnia, Membrane heat exchanger in HVAC energy recovery systems, systems energy analysis, Energy and Buildings 42 (2010) 1833–1840.
[14] A.K. Gholap, J.A. Khan, Design and multi-objective optimization of heat exchangers for refrigerators, Applied Energy 84 (2007) 1226–1239.
[15] A. Trząski, B. Zawada, The influence of environmental and geometrical factors on air-ground tube heat exchanger energy efficiency, Building and Environment 46 (2011) 1436–1444.
[16] R. Fan, Y.Q. Jiang, Y. Yao, D. Shiming, Z.L. Ma, A study on the performance of a geothermal heat exchanger under coupled heat conduction and ground water advection, Energy 32 (2007) 2199–2209.
[17] S. Ostrach, Natural convection in enclosures, Journal Heat Transfer 110 (1988) 1175–1190.
[18] T.S. Lee, Numerical experiments with fluid convection in tilted nonrectangular enclosures, Numerical Heat Transfer Part A 19 (1991) 487–499.
[19] B.V.R. Kumar, B. Kumar, Parallel computation of natural convection in trapezoidal porous enclosures, Math. Comput. Simulation 65 (2004) 221–229.
[20] A.C. Baytas, I. Pop, Natural convection in a trapezoidal enclosure filled with a porous medium, International Journal of Engineering Science 39 (2001) 125–134.
[21] F. Moukalled, S. Acharya, Natural convection in trapezoidal cavities with baffles mounted on the upper inclined surfaces, Numerical Heat Transfer Part A 37 (2000) 545–565.
[22] F. Moukalled, M. Darwish, Natural convection in a partitioned trapezoidal cavity heated from the side, Numerical Heat Transfer Part A 43 (2003) 543–563.
[23] M. Peric, Natural convection in trapezoidal cavities, Numerical Heat Transfer Part A 24 (1993) 213–219.
[24] J.T. Van Der Eyden, T.H. Van Der Meer, K. Hanjalic, E. Biezen, J. Bruining, Double-diffusive natural convection in trapezoidal enclosures, International Journal Heat Mass Transfer 41 (1998) 1885–1898.
[25] M. Boussaid, A. Djerrada, M. Bouhadef, Thermosolutal transfer within trapezoidal cavity, Numerical Heat Transfer Part A 43 (2003) 431–448.
[26] S. Kumar, Natural convective heat transfer in trapezoidal enclosure of box-type solar cooker, Renewable Energy 29 (2004) 211–222.
[27] E. Papanicolaou, V. Belessiotis, Double-diffusive natural convection in an asymmetric trapezoidal enclosure: unsteady behavior in the laminar and the turbulent-flow regime, International Journal Heat Mass Transfer 48 (2005) 191–209.
[28] M. Hammami, M. Mseddi, M. Baccar, Numerical study of coupled heat and mass transfer in a trapezoidal cavity, Eng. Appl. Comp. Fluid Dynamics 1 (2007) 216–226.
[29] Y. Varol, Natural convection in divided trapezoidal cavities filled with fluid saturated porous media, International Communication Heat Mass Transfer 37 (2010) 1350–1358.
[30] Y. Varol, H.F. Oztop, I. Pop, Numerical analysis of natural convection in an inclined trapezoidal enclosure filled with a porous medium, International Journal Thermal Science 47 (2008) 1316–1331.

[31] Y. Varol, H.F. Oztop, I. Pop, Entropy analysis due to conjugate-buoyant flow in a right-angle trapezoidal enclosure filled with a porous medium bounded by a solid vertical wall, International Journal Thermal Science 48 (2009) 1161–1175.
[32] Y. Varol, H.F. Oztop, I. Pop, Maximum density effects on buoyancy-driven convection in a porous trapezoidal cavity, International Communication Heat Mass Transfer 37 (2010) 401–409.
[33] E. Natarajan, T. Basak, S. Roy, Natural convection flows in a trapezoidal enclosure with uniform and non-uniform heating of bottom wall, International Journal Heat Mass Transfer 51 (2008) 747–756.
[34] T. Basak, S. Roy, A. Matta, I. Pop, Analysis of heatlines for natural convection within porous trapezoidal enclosures: effect of uniform and non-uniform heating of bottom wall, International Journal Heat Mass Transfer 53 (2010) 5947–5961.
[35] T. Basak, S. Roy, D. Ramakrishna, I. Pop, Visualization of heat transport due to natural convection for hot materials confined within two entrapped porous triangular cavities via heatline concept, International Journal Heat Mass Transfer 53 (2010) 2100–2112.
[36] T. Basak, G. Aravind, S. Roy, A.R. Balakrishnan, Heatline analysis of heat recovery and thermal transport in materials confined within triangular cavities, International Journal Heat Mass Transfer 53 (2010) 3615–3628.
[37] T. Basak, S. Roy, G. Aravind, Analysis of heat recovery and thermal transport within entrapped fluid based on heatline approach, Chemical Engineering Science 64 (2009) 1673–1686.
[38] H. Asan, L. Namli, Numerical simulation of buoyant flow in a roof of triangular cross-section under winter day boundary conditions, Energy & Buildings 33 (2001) 753–757.
[39] P.M. Haese, M.D. Teubner, Heat exchange in an attic space, International Journal Heat Mass Transfer 45 (2002) 4925–4936.